Large Isosymmetric Reorientation of Oxygen Octahedra Rotation Axes in Epitaxially Strained Perovskites

James M. Rondinelli[1,2,*] and Sinisa Coh[3]

[1]X-Ray Science Division, Argonne National Laboratory, Argonne, Illinois 60439, USA
[2]Department of Materials Science & Engineering, Drexel University, Philadelphia, Pennsylvania 19104, USA
[3]Department of Physics and Astronomy, Rutgers University, Piscataway, New Jersey 08854, USA

(Received 10 February 2011; published 10 June 2011)

Using first-principles density functional theory calculations, we discover an anomalously large biaxial strain-induced octahedral rotation axis reorientation in orthorhombic perovskites with tendency towards rhombohedral symmetry. The transition between crystallographically equivalent (isosymmetric) structures with different octahedral rotation magnitudes originates from strong strain-octahedral rotation coupling available to perovskites and the energetic hierarchy among competing octahedral tilt patterns. By elucidating these criteria, we suggest many functional perovskites would exhibit the transition in thin film form, thus offering a new landscape in which to tailor highly anisotropic electronic responses.

DOI: 10.1103/PhysRevLett.106.235502 PACS numbers: 61.50.Ks, 68.55.−a, 77.55.Px

Introduction.—Phase transitions are ubiquitous in nature; they describe diverse topics ranging from crystallization and growth to superconducting Cooper pair condensation. Isosymmetric phase transitions (IPT)—those which show no change in occupied Wyckoff positions or crystallographic space group—are an intriguing class since there are relatively few examples in crystalline matter [1]: Most condensed matter systems respond to external pressures and temperatures by undergoing ''conventional'' symmetry-lowering displacive [2], martensitic [3] or reconstructive [4] transitions. Furthermore, the experimental characterization and identification of a suitable symmetry-preserving order parameter through such transitions is often challenging [5]. Although some *electronic* order parameters [6,7] that include ferroelectric [8–11] or orbital polarizations [12] have been proposed for IPT, which lead to subsequent changes in local cation coordinations [13–15], to the best of our knowledge, there is no case where the IPT connects two structures with essentially the same local bonding environment.

Using first-principles density functional calculations, we find an isosymmetric transition in the low energy rhombohedral phases of epitaxially strained orthorhombic perovskites and describe how to experimentally access it. We show that the transition originates from nonpolar distortions that describe the geometric connectivity and relative phase of the BO_6 octahedra found in perovskites. Although a previous IPT in a thin film perovskite that relies on strong strain-polar phonon coupling has been reported [16], we describe here a universal symmetry-preserving transition that originates from the strong lattice-octahedral rotation coupling ubiquitous in nearly all perovskites. For this reason, the large isosymmetric reorientation of the oxygen rotation axes should be readily observable in many rhombohedral perovskites with diverse chemistries. Since the dielectric anisotropy in perovskites is strongly linked to deviations in the octahedral rotation axis direction [17], we suggest control over this transition could provide for highly tunable high-κ dielectric actuators and temperature-free relative permittivity resonance frequencies [18].

We choose $LaGaO_3$ as our model system since it has a tolerance factor of $\tau = 0.966$ indicating the perovskite structure is highly susceptible to GaO_6 octahedral rotations about the principle symmetry axes [19]: At room temperature it is orthorhombic *Pbnm* and undergoes a first-order phase transition to rhombohedral $R\bar{3}c$ around 418 K [20], with a subsequent change in the GaO_6 octahedral rotation patterns from $a^-a^-c^+$ to $a^-a^-a^-$, respectively, in Glazer notation [21]. The $+$ $(-)$ superscripts indicate in- (out-of)-phase rotations of adjacent octahedra along a given Cartesian direction. The nonmagnetic Ga^{3+} cations additionally allow us to eliminate possible contributions of spin and orbital degrees of freedom for driving the IPT through electronic mechanisms.

Calculation details and notation.—Our density functional calculations are performed within the local density approximation (LDA) as implemented in the Vienna *ab initio* simulation package (VASP) [22,23] with the projector augmented wave (PAW) method [24], a $5 \times 5 \times 5$ Monkhorst-Pack k-point mesh [25] and a 500 eV plane wave cutoff. We relax the atomic positions (forces to be less than 0.1 meV Å^{-1}) and the out-of-plane c-axis lattice constants for the strained films [26].

The principle difference between the ground state orthorhombic *Pbnm* and metastable [12 meV per formula unit (f.u.) higher in energy] rhombohedral $R\bar{3}c$ phases of $LaGaO_3$ is that the GaO_6 octahedra rotate in-phase $(+)$ along the Cartesian z direction of the *Pbnm* structure while they rotate out-of-phase $(-)$ about that same direction in the $R\bar{3}c$ structure. Our homoepitaxial biaxial strain calculations simulate film growth on a cubic (001)-terminated substrate. We therefore choose the c^+ rotations of the

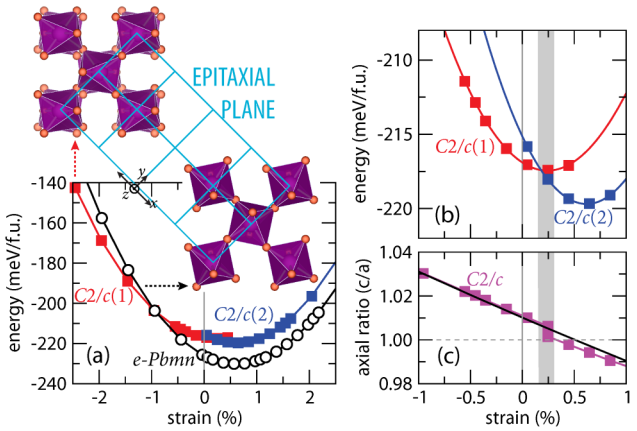

FIG. 1 (color online). Evolution of the total energy (a) for the *e-Pbnm* and $C2/c$ phases with in- and out-of-phase octahedral rotations (inset) along the z direction. (b) Magnified region about the IPT (shaded). (c) The change in axial ratio with strain shows a discontinuity in the $C2/c$ phase that is absent in the *e-Pbnm* structure.

orthorhombic phase to be about the axis perpendicular to the epitaxial plane (Fig. 1), to evaluate the biaxial strain effect on the in- versus out-of-phase GaO_6 rotations present in the two phases. Note, the biaxial constraint preserves the orthorhombic symmetry in the $a^-a^-c^+$ phase; however, we designate the *epitaxially* (*e*) strained phase as *e-Pbnm* to distinguish it from the bulk structure. In contrast, the symmetry of the bulk rhombohedral phase is lowered to monoclinic (space group $C2/c$) and we therefore refer to it as such [27].

Strain-stabilized structures.—We first compute the evolution in the total energy with biaxial strain for the *e-Pbnm* and $C2/c$ structures [Fig. 1(a)]. We find that between approximately -1 to $+3\%$ strain, the orthorhombic phase with the $a^-a^-c^+$ rotation pattern is more stable than the monoclinic $a^-a^-c^-$ structure. For now we focus on the monoclinic phases [Fig. 1(b)] near 0% strain: We find an abrupt discontinuity in the first derivative of the total energy with strain for the monoclinic structure between two states with the same symmetry, denoted $C2/c(1)$ and $C2/c(2)$. In contrast, we find a single continuous equation of state with *uniform* hydrostatic pressure (over ± 50 GPa) for the bulk structures. The evolution in the c/a axial ratio for these structures is also qualitatively different [Fig. 1(c)]. The *e-Pbnm* axial ratio continuously decreases with increasing tensile strain (consistent with elastic theory), whereas in the $C2/c$ structures a sharp discontinuity occurs in the vicinity of $c/a \sim 1$. We find the first-order phase transition occurs at a critical strain of $\sim 0.18\%$ from intersection of the quadratic fits to the total energies.

Microscopic structure evolution.—To investigate if the $C2/c(1) \rightarrow C2/c(2)$ transition is indeed isosymmetric, we evaluate how the internal structural parameters—octahedral tilts and bond distortions—evolve with epitaxial strain [Fig. 2(a)]. We find a continuous evolution in the GaO_6 rotation angles for the *e-Pbnm* structures (open symbols): the rotation axis changes from being along the [001] direction to mainly in plane along [110] as the strain state changes from compressive to tensile. In contrast, we find an abrupt change in the octahedral rotation angles with strain in the monoclinic phases (filled symbols). We identify that the $C2/c(1)$ and $C2/c(2)$ phases, despite possessing the same symmetry are distinguishable—they have either mainly [110] in-plane or [001] out-of-plane GaO_6 octahedra rotations. Consistent with the orthorhombic case we find that increasing tensile strain drives the octahedral rotation axis into the [110]-epitaxial plane.

The biaxial strain is not solely accommodated by rigid octahedral rotations. It produces additional deviations in the Ga-O bond lengths and causes La cation displacements. We quantify the former effect through the octahedral distortion parameter $\Delta = \frac{1}{6}\sum_{n=1,6}[(\delta(n) - \langle\delta\rangle)/\langle\delta\rangle]^2$, where δ is a Ga-O bond length and $\langle\delta\rangle$ is the mean bond length in the GaO_6 octahedra. With increasing strain, Δ increases, indicating that bond stretching (and compression) occurs simultaneously with changes in the magnitude of the octahedral rotation angles to alleviate the substrate-induced strain [Fig. 2(b)]. According to our bond-valence calculations, the Ga-O bond stretching alleviates the "chemical strain" imposed on the over-bonded Ga^{3+} cations when a regular GaO_6 octahedra ($\Delta \rightarrow 0$) occurs. The IPT allows the monoclinic phase to maintain a uniform charge density distribution with the $a^-a^-c^-$ tilt pattern; this is assisted by the antiparallel La displacements [Fig. 2(c)], which change sign across the transition (shaded), maintaining a trigonal planar configuration in the GaO_6 rotation-created cavities. Note, this chemically overbonded structure is absent in the

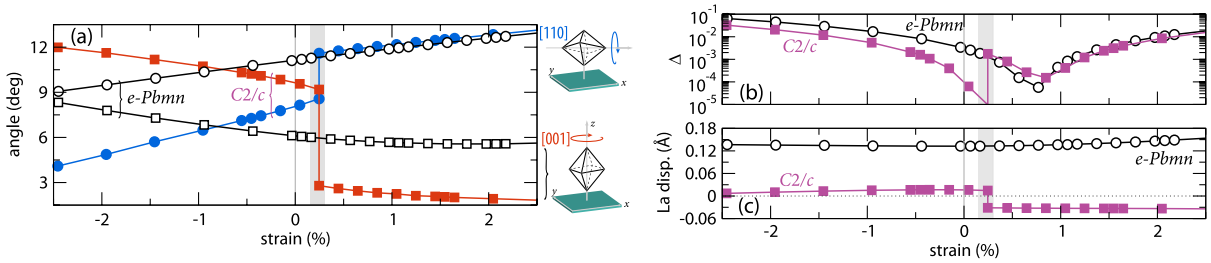

FIG. 2 (color online). Evolution in (a) the GaO_6 rotation angles about different directions relative to the substrate, (b) the octahedral distortion parameter Δ, and (c) the La displacements about the bulk structures with epitaxial strain.

e-Pbnm structure because the $a^-a^-c^+$ tilt pattern (D_{2h} symmetry) permits nonuniform Ga-O bonds. Since the rotation pattern never reverses, a single La cation displacement direction occurs.

Origin of the IPT.—To identify the origin of the isosymmetric transition, we first analyze the energy of the monoclinic $a^-a^-c^-$ structures under different biaxial strain states as a function of *direction* and *magnitude* of the GaO_6 octahedron rotation axis. The direction of the GaO_6 rotation axis with the $a^-a^-c^-$ pattern is constrained to be in the $(\bar{1}10)$-plane because the rotation pattern can be decomposed into $a^-a^-c^0$ and $a^0a^0c^-$ rotations with axes aligned along the [110] and [001] directions [Fig. 2(a)]. We show in Figs. 3(a)–3(c) our first-principles results of the energy dependence on the direction (vertical axes) and magnitude (horizontal axes) of the GaO_6 rotation axis for strain values of −1.5%, 0.0% and 1.5%, respectively. For all strain states, we find a single well-defined energy minimum for each *direction* of the GaO_6 rotation axis [Figs. 3(a)–3(c)]. We therefore are able to remove the rotation angle magnitude as a variable and to analyze the energy dependence solely in terms of the biaxial strain and the GaO_6 rotation axis *direction* [28].

We show in Fig. 3(d) the calculated evolution of the extremal octahedra rotation axis directions with biaxial strain: local energy minima (maxima) are indicated with a heavy (broken) line, and for −1.5%, 0.0%, and 1.5% biaxial strains, we explicitly mark the extrema using symbols. Consistent with our earlier structural analysis, we find

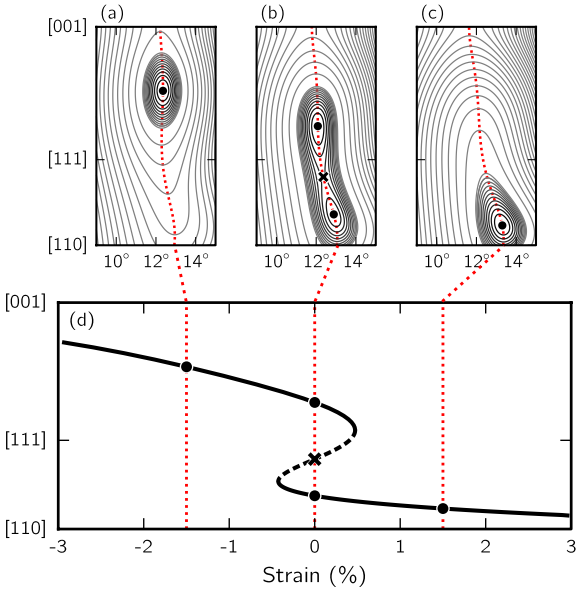

FIG. 3 (color online). Calculated energy (a)–(c) of the monoclinic $LaGaO_3$ phases as a function of the GaO_6 rotation axis direction and angle magnitude at −1.5%, 0.0% and 1.5% strains, respectively, with contours at 5 and 0.5 meV/f.u. (d) Position of energy minimum (solid line) or maximum (broken line) with strain; circles correspond to minima (a)–(c), and the cross indicates the saddle point in (b).

that the rotation axis direction smoothly approaches the [110]- ([001]-) direction for large tensile (compressive) strains. For the range of strains between −0.5% and 0.5%, we observe the coexistence of two energy minima separated by an energy maximum (broken line); this indicates an *inaccessible region* of rotation axis directions close to [111] for any value of strain and is consistent with a first-order transition.

Our results suggest there are two main reasons for the appearance of the isosymmetric transition in epitaxially strained rhombohedral perovskites. The first reason is that the octahedral rotations are strongly coupled to the biaxial strain. This coupling originates from the rigidity of the GaO_6 octahedra, since the rigidity causes contraction of the crystal lattice in the direction orthogonal to the rotation axis [29,30]. Second, the bulk rhombohedral $a^-a^-a^-$ structure of $LaGaO_3$ is *higher* in energy than the bulk orthorhombic $a^-a^-c^+$ structure.

We now show that the energy ordering of the bulk phases is responsible for the *inaccessible region* of rotation axis directions. The $a^-a^-a^-$ and $a^-a^-c^+$ structures differ only in the phase of the GaO_6 octahedra rotations about the z axis. Thus, each structure can be transformed into the other through a combination of rigid octahedral distortions. One distortion should deactivate the a^- rotation about the z axis, while the other would induce the c^+ rotation about the same axis. We would expect these distortions to impose minor energetic penalties since they are nearly rigid [31]. In the present case, where the $a^-a^-a^-$ structure is higher in energy than $a^-a^-c^+$, we expect that introduction of either of these distortions into the *higher* energy $a^-a^-a^-$ structure will lower the total energy [32].

Finally, smoothness of the total energy as a function of strain and rotation axis direction requires that the difference between the number of energy minima ($N_{\min}$) and maxima ($N_{\max}$), for any value of biaxial strain, remains fixed as elaborated in Morse theory [28]. In other words, any smooth deformation which produces additional energy maximum must also produce additional energy minimum. Because of the first reason for the IPT mentioned above, we anticipate that for sufficiently large compressive or tensile strains, the strain-octahedral rotation direction coupling dominates to yield a single energy minimum: $N_{\min} = 1$, $N_{\max} = 0$ and then from continuity, $N_{\min} - N_{\max} = 1$ must remain constant for all strains. From our energetic hierarchy of the bulk structures, we conclude that when strain induces structural distortions with magnitudes which nearly coincide with those of the bulk $a^-a^-a^-$ phase (near 0% strain and [111] direction), there will exist an energy maximum ($N_{\max} = 1$); from continuity, this must introduce two energy minima ($N_{\min} = 2$) at the same value of strain. These reasons together produce the energy landscape shown in Fig. 3(d) and require an IPT in the $LaGaO_3$ system. For comparison, the orthorhombic phase of $LaGaO_3$ does not show an IPT as one varies biaxial strain, since the second condition for the transition described above does not apply, i.e., the orthorhombic

structure is the global ground state: $N_{\min}$ is fixed to 1 ($N_{\max} = 0$) for all strain values.

Accessing and applications of the IPT.—We obtain a $C2/c \rightarrow e\text{-}Pbmn$ transition near -1% compressive strain with respect to our hypothetical cubic $LaGaO_3$ phase. In the vicinity of the IPT at 0 K, however, the *e-Pbmn* phase is the global ground state. Although our minimal model for the IPT relies on this energetic ordering of the competing rotational phases ($a^-a^-a^-$ versus $a^-a^-c^+$), we anticipate three experimental routes by which to access the essential signature of the isosymmetric transition—large strain-induced reorientation of the octahedral rotation axis direction. First, the monoclinic phases could be stabilized in thin films through the substrate coherency effect [33], where the film's tilt pattern adopts that of the substrate: Perovskite substrates with the $a^-a^-a^-$ ($LaAlO_3$) or the $a^0a^0c^-$ (tetragonal-$SrTiO_3$) tilt pattern are promising candidates. Second, additional electronic degrees of freedom (first- and second-order Jahn-Teller effects), introduced through cation substitution, could be exploited to stabilize the IPT because they often energetically compete with the octahedra rotations [34]. Lastly, experiments performed above the bulk $LaGaO_3$ structural transition temperature ($\sim 100\,^\circ$C) would make the monoclinic phases accessible at all strains. The IPT would exhibit a weak-first-order transition while still providing strong strain-octahedral rotation axis direction coupling. At sufficiently high temperatures, the IPT could be suppressed and its boundary terminated by a critical point [35].

We have shown that strain-octahedral rotation axis directions are strongly coupled in epitaxial perovskite thin films. We suggest similar large reorientations of coordinating polyhedra frameworks could be achieved in alternative structural families: thin films with the garnet, apatite or spinel structures are particularly promising. However, the functional materials design challenge remains: how does one couple the rotation axis direction to additional *electronic* degrees of freedom? For this reason, we advocate for detailed epitaxial film studies on perovskites close to the $R\bar{3}c \leftrightarrow Pnma$ phase transition ($0.96 < \tau < 1.01$). Controlling the IPT in $LaCrO_3$, $LaNiO_3$ and $LaCuO_3$ perovskites could yield unknown, and potentially functional, orbitally-, spin-, and charged-ordered phases.

J. M. R. thanks S. May, C. Fennie and L. Marks for discussions and support from U.S. DOE under Contract No. DE-AC02-06CH11357. S. C. thanks D. Vanderbilt and M. H. Cohen for useful discussions and Rutgers-Lucent Fellowship for support.

*jrondinelli@coe.drexel.edu

[1] R. A. Cowley, Phys. Rev. B **13**, 4877 (1976).
[2] W. Cochran, Phys. Rev. Lett. **3**, 412 (1959).
[3] A. Khachaturyan, *Theory of Structural Transformations in Solids* (Wiley, New York, NY, 1983).
[4] P. Tolédano and V. Dimitrev, *Reconstructive Phase Transitions in Crystals and Quasicrystals* (World Scientific, Singapore, 1996).
[5] A. G. Christy, Acta Crystallogr. Sect. B **51**, 753 (1995).
[6] A. W. Lawson and T.-Y. Tang, Phys. Rev. **76**, 301 (1949).
[7] R. Caracas and X. Gonze, Phys. Rev. B **69**, 144114 (2004).
[8] J. F. Scott, Adv. Mater. **22**, 2106 (2010).
[9] R. J. Zeches *et al.*, Science **326**, 977 (2009).
[10] S. Tinte, K. M. Rabe, and D. Vanderbilt, Phys. Rev. B **68**, 144105 (2003).
[11] J. S. Tse and D. D. Klug, Phys. Rev. Lett. **81**, 2466 (1998).
[12] K. Friese, Y. Kanke, A. N. Fitch, and A. Grzechnik, Chem. Mater. **19**, 4882 (2007).
[13] I. P. Swainson, R. P. Hammond, J. K. Cockcroft, and R. D. Weir, Phys. Rev. B **66**, 174109 (2002).
[14] J. Haines, J. M. Léger, and O. Schulte, Phys. Rev. B **57**, 7551 (1998).
[15] S. Carlson, Y. Xu, U. Halenius, and R. Norrestam, Inorg. Chem. **37**, 1486 (1998).
[16] A. J. Hatt, N. A. Spaldin, and C. Ederer, Phys. Rev. B **81**, 054109 (2010).
[17] S. Coh *et al.*, Phys. Rev. B **82**, 064101 (2010).
[18] E. L. Colla, I. M. Reaney, and N. Setter, J. Appl. Phys. **74**, 3414 (1993).
[19] P. M. Woodward, Acta Crystallogr. Sect. B **53**, 44 (1997).
[20] C. J. Howard and B. J. Kennedy, J. Phys. Condens. Matter **11**, 3229 (1999).
[21] A. M. Glazer, Acta Crystallogr. Sect. B **28**, 3384 (1972).
[22] G. Kresse and J. Furthmuller, Phys. Rev. B **54**, 11 169 (1996).
[23] G. Kresse and D. Joubert, Phys. Rev. B **59**, 1758 (1999).
[24] P. E. Blöchl, Phys. Rev. B **50**, 17 953 (1994).
[25] H. J. Monkhorst and J. D. Pack, Phys. Rev. B **13**, 5188 (1976).
[26] All strain values are given relative to the hypothetical cubic equilibrium LDA lattice parameter (3.831 Å).
[27] In the monoclinic structures, we constrain the free interaxial angle to be that of the fully relaxed rhombohedral structure following Ref. [16].
[28] D. Vanderbilt and M. H. Cohen, Phys. Rev. B **63**, 094108 (2001).
[29] S. J. May *et al.*, Phys. Rev. B **82**, 014110 (2010).
[30] A. J. Hatt and N. A. Spaldin, Phys. Rev. B **82**, 195402 (2010).
[31] If a change in the $a^-a^-a^0$ rotation also occurs, so as to keep the total octahedron rotation angle magnitude nearly constant, the energy penalty is even smaller and fully consistent with the energy landscape in Figs. 3(a)–3(c).
[32] We calculate two unstable phonons ($\omega = 25i$ cm^{-1} and $43i$ cm^{-1} at the zone-center and zone-boundary, respectively) in the rhombohedral structure corresponding to these kind of distortions.
[33] J. M. Rondinelli and N. A. Spaldin, Phys. Rev. B **82**, 113402 (2010).
[34] T. Mizokawa, D. I. Khomskii, and G. A. Sawatzky, Phys. Rev. B **60**, 7309 (1999).
[35] Y. Ishibashi and Y. Hidaka, J. Phys. Soc. Jpn. **60**, 1634 (1991).